Available online at www.sciencedirect.com

ScienceDirect

Procedia Structural Integrity 8 (2018) 137–153

Structural Integrity Procedia

www.elsevier.com/locate/procedia

AIAS 2017 International Conference on Stress Analysis, AIAS 2017, 6-9 September 2017, Pisa, Italy

Numerical FEM Evaluation for the Structural Behaviour of a Hybrid (bonded/bolted) Single-lap Composite Joint

E. Armentani[a]*, M. Laiso[b], F. Caputo[b], R. Sepe[a]

[a]*Dept. of Chemical, Materials and Production Engineering, University of Naples Federico II, P.le V. Tecchio 80, 80125 Naples, Italy*
[b]*Dept. of Industrial and Information Engineering, Università della Campania "Luigi Vanvitelli", Via Roma 29, 81031 Aversa, Italy*

Abstract

The structural behaviour of a single-lap hybrid (bonded/bolted) composite joint subjected to a tensile external load was evaluated by means of the Finite Element Method (FEM). In particular, the distribution of stresses acting in its adhesive layer was compared with that relative to the case of a simply adhesive bonded joint. Furthermore, the load transferred by the bolt was determined at different characteristics of the adhesive and of the applied external tensile load, corresponding to both single and double bolt configuration. The obtained values were in turn compared with experimental data found in literature, so validating the produced numerical simulations.

Peer-review under responsibility of the Scientific Committee of AIAS 2017 International Conference on Stress Analysis

Keywords: hybrid joint; composites; FEM; ANSYS®; adhesive; bonded; bolted; HI-LOK™; Drucker-Prager yield criterion

1. Introduction

In many industrial sectors, particularly aerospace, develop and use of composite materials is very relevant. These materials allow the production of goods relatively complex and of big dimensions, the use of joints results to be always necessary for creating complex structures. Traditionally joints between composite materials were made by a mechanical fastening, however this technique shows various disadvantages such as high stress concentrations at the

* Corresponding author. Tel.: +39-081-768-24-50; fax: +39-081-768-24-52.
E-mail address: enrico.armentani@unina.it

Peer-review under responsibility of the Scientific Committee of AIAS 2017 International Conference on Stress Analysis
10.1016/j.prostr.2017.12.015

hole, also due to a localised load transfer, which reduces considerably the fatigue and fracture strength of the joint. For this reason, the adhesive bonding technique is preferred in the joining of composite material parts. By this technique the load can be transferred in a continuous manner allowing a better stress distribution. Furthermore, the absence of holes in such joining of composites avoids the deterioration of mechanical characteristics and structural integrity due to fibres cut.

In many cases adhesive bonded joints are reinforced through the use of rivets. Traditionally the combination of mechanical fastening and adhesive bonding was considered useless in order to structural performance. However, the evaluations here made are aimed to the study of high performance aerospace joints, characterized by high modulus epoxy resin adhesives. In this case the adhesive layer transfers most of the load, without having appreciable benefits in the performance adding bolts. In fact, only by using a low modulus adhesive a better load distribution between bolt and adhesive was obtained, giving to the joint a greater strength, stiffness and fatigue life. Moreover, the use of the bolt allowed to avoid premature joint fractures due to defects inside the adhesive and allowed the alignment of the structures to be joined during the adhesive cure cycles (Kelly (2006)).

In the present work numerical analyses by Finite Element Method (FEM), for the evaluation of the structural performance of a single-lap hybrid joint subjected to an external tensile load were made. In particular, by means of the software ANSYS®, the stress distribution acting on the adhesive was determined and compared with that relative to a simply adhesive bonded joint. Moreover, the load transferred by the bolt was estimated for varying adhesive characteristics and applied load, with one or two bolts. These results were then compared to the experimental ones for the validation of the numerical simulation.

Kelly (2005) analysed the load distribution in hybrid composite single-lap joints through 3D FEM including the effects of bolt-hole contact and non-linear material behaviour. By means of a parametric study, he investigated the effect of joint design parameters on the load transferred by the bolt. Moreover, a joint was experimentally equipped with an instrumented bolt, used to measure the load transfer in the joint. Measured bolt load values were compared to predictions from FEM and results showed good agreement. Kelly (2006) continued the previous work focusing on strength and fatigue life of hybrid (bonded/bolted) joints with CFRP (Carbon Fiber Reinforced Polymers) adherends. He determined experimentally the effect of adhesive material properties and laminate stacking sequence on joint's structural behaviour and failure modes. Hybrid joints with lower modulus adhesives showed greater strength, stiffness and fatigue life in comparison to simply adhesive bonded joints. Hybrid joints with high modulus adhesives showed no significant improvement in strength although increased fatigue life was observed due to the presence of the bolt. Ireman (1998) made a 3D FEM analysis of bolted composite joints to determine non-uniform stress distributions through the thickness of composite laminates in the vicinity of a bolt hole. Experimental elongations, strains, and bolt load on test specimens were measured to validate the numerical model and a number of parameters such as laminate layup and thickness, bolt diameter and type, clamping force and lateral support was varied, each analysed by using a 3D FEM. Generally, comparison between computed and experimental results showed good agreement. Barut and Madenci (2009) developed a semi-analytical solution method for stress analysis of single-lap hybrid (bolted/bonded) joints of composite laminates under in-plane and lateral loading. The laminate and bolt displacements were based on the Mindlin and Timoshenko beam theories, respectively. Adhesive displacement field was expressed in function of those of laminates by using the shear-lag model. Governing equilibrium equations were based on the virtual work principle. The capability of the approach was validated by demonstration problems, including the analysis of bolted and bonded joints and hybrid joints with and without considering a dis-bond between adhesive and laminates. Paroissien et al. (2007) presented two 1D elastic analytical models for the determination of the load transfer in a hybrid (bolted/bonded) single-lap joint. The first one developed the integration of the local equilibrium equations with an elastic-plastic approach. The second one used the FEM, introducing a new element called "bonded-bar". The two approaches allowed to analyse the load transfer and to evaluate the influence of different geometric and mechanical parameters. Hart-Smith (1985) considered the combination of adhesive bonding and mechanical fastening for fibrous composite structures. Analyses of undamaged structures showed that, because the adhesive bond load path is so much stiffer than the load path through bolts or rivets, the combination was not stronger than a well-designed bonded joint alone. However, the combination of bonding and bolting seemed to be useful for repair and prevent damage from spreading of plates. Studies involved large stepped-lap composite to metal joints. Imanaka et al. (1995) investigated the strength characteristics of adhesive/rivet combined lap joints. They made fatigue tests on rivet, adhesive and adhesive/rivet combined joints with different lap widths, adhesive and rivet

strengths. Furthermore, to compare fatigue crack initiation and propagation behaviour of the adhesive joint with those of the combined joint, the strain changes were measured by strain gauges bonded onto the adherend plate near the lap end. Fatigue strength of adhesive joints could be improved by combining the adhesive with rivets of nearly equal or slightly higher fatigue strength than the adhesive joint. Furthermore, fatigue cracks propagated more gradually in combined joints than in adhesive joints after crack initiation. Crocombe et al. (2002) made numerical studies for investigating the effect of key parameters on the joining technique and to determine optimum gauge specification and location. They made calibration curves relative to strain change due to the extent of damage. These numerical studies were then validated through a series of fatigue tests on both aluminium and GRP-bonded joints. Predicted and observed damage showed close correlation. Fatigue tests also indicated that, for unmodified joints (intact fillets), even at high loads (50% static failure loads), there was an initiation phase that accounted for about a half the fatigue life of the joint. Removal of the adhesive fillet eliminated the initiation phase and consequently reduced the fatigue life. McCarthy et al. (2002) investigated the effects of bolt-hole clearance on the stiffness and strength of composite bolted joints. They studied single-lap/single-bolt joints. Four different clearances were considered, ranging from neat-fit to 240 mm. Both protruding head and countersunk bolts were used, with two different applied torque levels. Specimen dimensions were chosen to obtain bearing as primary failure mode. Increasing clearance resulted in reduced joint stiffness and increased ultimate strain in all tested configurations. Finger-tight joints with protruding head bolts showed a link between clearance and strength, but countersunk and torqued joints did not. A delay in load take-up also occurred with the higher clearance joints, which affected the load distributions in multi-bolt joints. Barroso et al. (2010) analysed an adhesive double-lap joint between unidirectional carbon-epoxy composite and aluminium plates. An elasto-plastic FEM simulation determined the extent of the yielded zone at the neighbourhood of the bi-material corner appearing at the end of the overlap and was compared with the purely elastic solution. Results showed that the yielding zone appeared around the corner with a significant influence from the used yielding criteria. Three yielding criteria were considered taking or not into account the influence of the mean stress: Raghava, Drucker-Prager and Von Mises. The results with the different yielding criteria were compared with the analytical (elastic) and numerical elastic (boundary element) solutions. The comparison with experimental results suggested that the most suitable criterion had to be dependent on the mean stress. De Luca et al. (2016) made a FEM analysis to determine the stress-strain state for a bonded single lap joint under peeling load. The method was validated by comparing the numerical results with the experimental ones and a good correlation was achieved. Moreover, the adhesive layer was modelled by means of cohesive elements which, however, present some numerical difficulties, related to the dependence from the own element size, and hence solved through a proper procedure.

2. Geometry and material

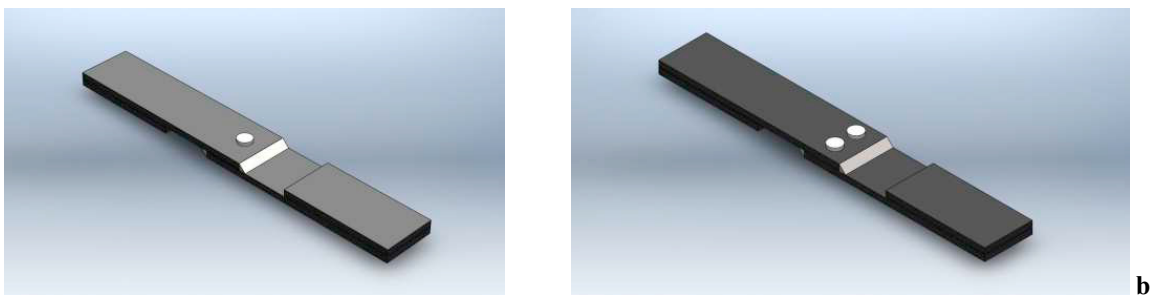

a **b**

Fig. 1. (a) Single-lap joint with one bolt; (b) single-lap joint with two bolts.

The single-lap joint was modelled with two adherends of length and width equal to 90 mm and 25 mm respectively, with an overlap of 20 mm. At the interface of the two laminates there was placed an adhesive layer of

thickness of 0.5 mm; at the ends of the plates the adhesive layer has been closed with a 45° fillet. At the centre of the overlap a 6.35 mm diameter hole was made to introduce a HI-LOK^{TM} with head and collar equal to 10 mm of diameter. In the case of double bolt configuration, the HI-LOK^{TM} bolts were spaced 12.5 mm. Fig. 1 shows the two configurations of the joint. These dimensions were given in parametric form as pointed out by the following Fig. 2 and Table 1:

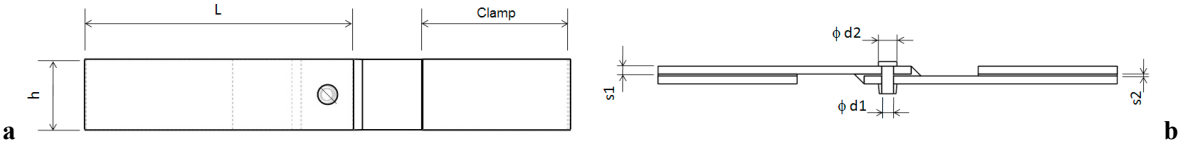

Fig. 2. (a) Top view and (b) side view of the single-lap joint.

Table 1. Characteristic dimensions of the single-lap joint.

Symbol	Meaning	Value
h	Width of the adherend	25 mm
L	Length of the adherend	90 mm
d1	Diameter of the pin shank	6 mm
d2	Diameter of the pin head	10 mm
Clamp	Clamping length of the machine	30 mm
s1	Thickness of the adherend	4.16 mm
s2	Thickness of the adhesive	0.5 mm

The two laminates were made with a prepreg carbon fibre with epoxy resin with 32 laminae stacked by the sequence $[\pm 45/90/0]_{4s}$. The characteristics of the single lamina are given in Table 2 and taken from Kelly (2005):

Table 2. Mechanical characteristics of the single lamina.

Mechanical parameter	Value
E_{11}	140 GPa
E_{22}	10 GPa
E_{33}	11 GPa
G_{12}	5.2 GPa
G_{13}	5.2 GPa
G_{23}	3.9 GPa
ν_{12}	0.3
ν_{13}	0.3
ν_{23}	0.5

The adhesive considered was Pliogrip 7400/7410 (Ashland Speciality Chemicals GmbH) which is a two structural components polyurethanic resin with a low elastic modulus (E = 600 MPa) and a large strain to failure. The tensile stress-strain behaviour of the adhesive are reported in Kelly (2005). The elasto-plastic properties of the adhesive material were modelled using the Drucker-Prager yield criterion.

The HI-LOK^{TM} pin was made of titanium with a collar of titanium. The elastic mechanical properties are E = 110 GPa and ν = 0.34.

3. Numerical model

3.1. Adherends

The numerical model was made by means of code ANSYS® using ANSYS Parametric Design Language (APDL) so that each geometric characteristic of the specimen can be modified easily by only changing the values assumed by parameters in the input text file and indicated in Table 1.

The adherends were modelled by the element SOLID185 which is defined by eight nodes having three translational degrees of freedom at each node and allows assigning the stacking sequence of the laminate. The overlap zone with a hole lodging the bolt was discretized with local different densities for appreciating the local different stress and deformation states (Fig. 3). First a ring with a fine mesh in correspondence of head and collar of the bolt, then a transition mesh towards a coarse mesh for the remaining part of the overlap zone. In the same manner the remaining part of the adherend had a finer mesh near the overlap zone then a coarser mesh in the zones clamped by the machine.

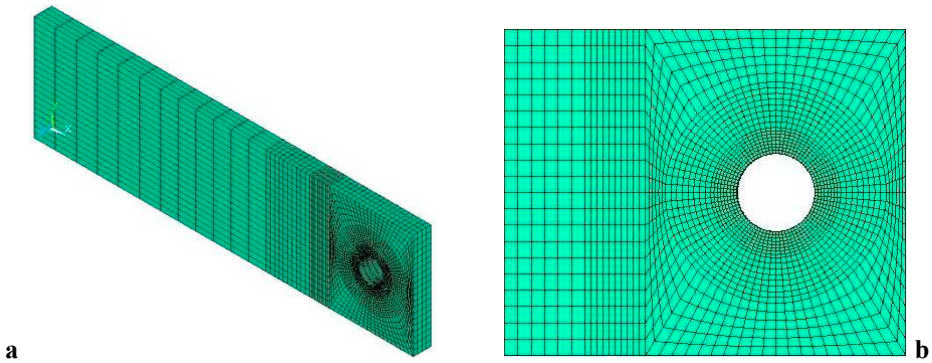

Fig. 3. Mesh of the adherend: (a) complete and (b) particular of the overlap zone.

3.2. Adhesive

The adhesive was modelled by SOLID65 which is a usual solid element defined by eight nodes having three translational degrees of freedom at each node. This element was used for implementing the adhesive elasto-plastic behaviour following the linear criterion of Drucker-Prager. Fig. 4 shows the whole adhesive volume mesh at the overlap zone.

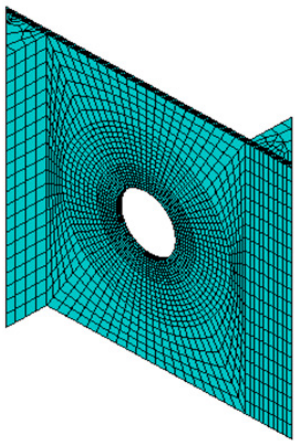

Fig. 4. Mesh of the adhesive volume at the overlap zone.

3.3. Bolt and collar

The model of HI-LOK^{TM} bolt and corresponding collar were made with the already used element SOLID185. Fig. 5a shows how the mesh of the bolt axially equals those of the two adherends and of the adhesive layer and how that of the head also equals that of mesh around the holes. The collar is a simple truncated circular cone (Fig. 5b) with a mesh following that of bolt's shank.

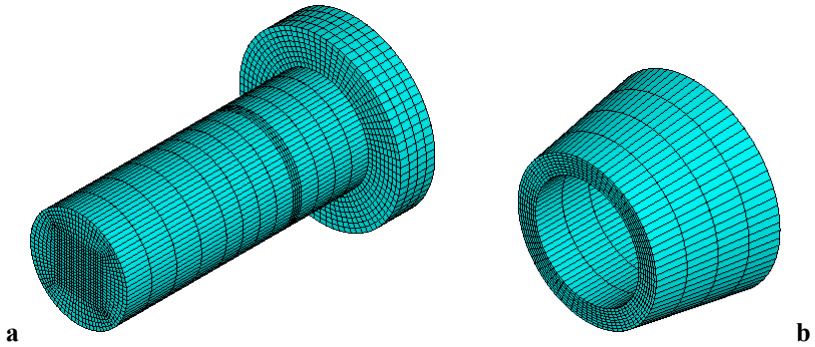

Fig. 5. Mesh of (a) bolt and (b) collar.

When a bolt is applied to make a joint, it is subjected to a preload. In ANSYS® this is made through a "pretension section" made by cutting the mesh of the bolt in two parts having two node planes geometrically coincident but with nodes physically distinct. These two node planes are linked by a pretension element (PRETS179). This element has only one translational degree of freedom along the preload direction, where the user can apply the desired pretension load as force or displacement on the bolt and then on the overlap zone.

3.4. Contacts

For studying the behaviour of a hybrid joint it is mandatory the analysis of contacts occurring between adherends and bolt. In this study the surface-to-surface contact of the type flexible-to-flexible was used. The elements TARGE170 and CONTA173 were used for the target surface and for the impacting surface respectively. The following Fig. 6 shows the two types of surfaces with the corresponding normal.

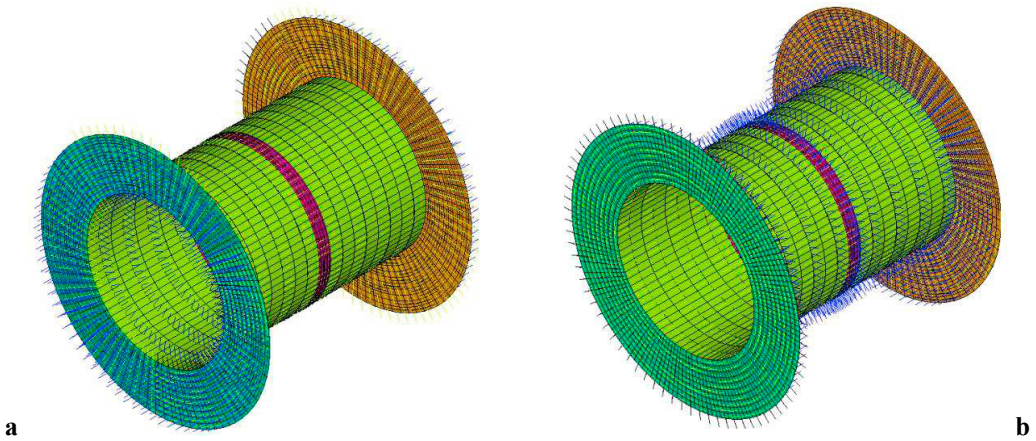

Fig. 6. (a) Target elements with their normal; (b) contact elements with their normal.

The element CONTA173 needed the definition of the friction characteristics. In this case an isotropic Coulomb friction was used with a friction coefficient $\mu = 0.2$.

3.5. Constraints and loads

For simulating the experimental tensile test made by a universal testing machine, proper constraints and loads were applied on the numerical model. An end of the specimen was kept blocked by the machine and hence the nodes

corresponding to the clamped part were characterized by constraints forbidding all of the three displacements (the cyan triangles on the left side laminate in Fig. 7). The other end was able to move exclusively in the longitudinal direction (*x*-direction) during the test hence the nodes corresponding to its clamped part had displacements forbidden in *y*- and *z*-direction (the cyan triangles on the right side laminate in Fig. 7), whereas the applied external load acting in *x*-direction was applied. Indeed, a concentrated load was applied to only one node suitably made and then it was transferred on the proper nodes (the magenta lines in Fig. 7).

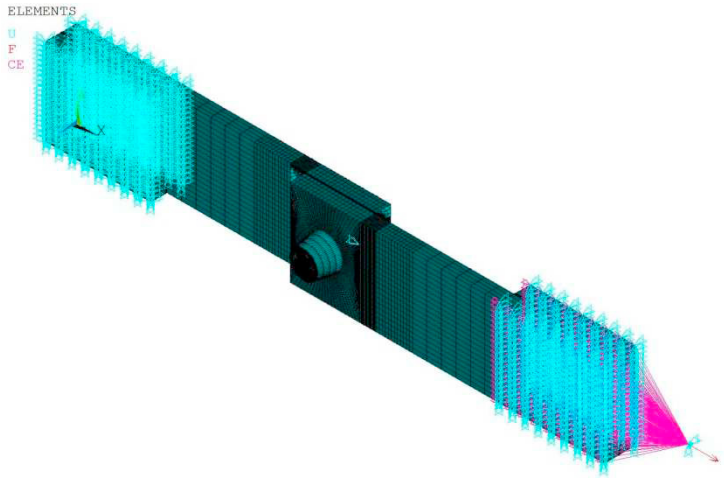

Fig. 7. Constraint and load systems.

4. Results

All of the following figures representing displacements, stresses, strains, etc. are related to the case of an applied external load of 3000 N.

The numerical analysis is non-linear because of:

- the presence of contacts;
- the hypothesis of great displacements;
- the adhesive material non-linear behaviour.

As regards to the non-linear behaviour of the adhesive, the Drucker-Prager criterion was used. It differs from the Von Mises criterion for the introduction of the material sensitivity as regards to the hydrostatic stress component. In particular, this criterion is expressed by the formulation:

$$f = \sqrt{3 j_2} + \alpha \sigma_m - \sigma_y = 0 \tag{1}$$

where α is the pressure sensitivity parameter and it is equal to:

$$\alpha = \frac{6 \sin \phi}{(3 - \sin \phi)} \tag{2}$$

where ϕ is the internal friction angle. The term $\sqrt{3j_2}$ corresponds to the equivalent Von Mises stress, whereas σ_m and σ_y corresponds to the hydrostatic stress and tensile yielding stress respectively.

The parameters required by ANSYS® for using this criterion are:

$$c = \frac{\xi \sigma_y}{\sqrt{6\xi - 2}} \tag{3}$$

$$\sin\phi = \frac{3(\xi - 1)}{3\xi + 1} \tag{4}$$

where ξ is defined as the ratio between tensile and shear yielding limits through:

$$\frac{\sigma_y}{\tau_y} = \frac{\sqrt{3}(\xi - 1)}{2\xi} \tag{5}$$

In this case, by having used an adhesive with yielding limits equal to σ_y = 10 MPa and τ_y = 6 MPa, these values were used: c = 5.10 and ϕ = 3.30 degree.

4.1. Deformations

The asymmetry of the joint geometry caused an eccentricity of the applied loads, causing in turn a rotation of the joint at the overlap zone (Fig. 8).

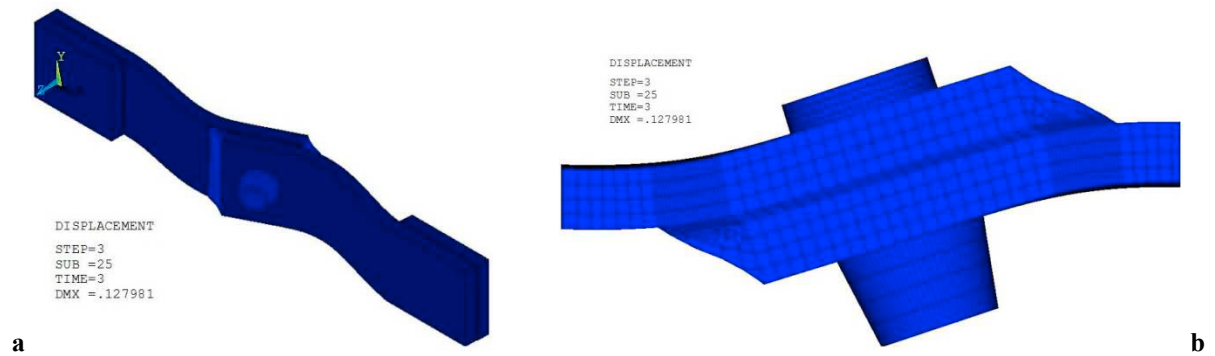

Fig. 8. (a) Deformation of the whole joint; (b) particular of the overlap zone (always for an applied external load of 3000 N).

Displacements are shown in the following Fig. 9, represented over the undeformed shape.

4.2. Stresses

The stress field in the adherend is generally dependent on the tensile applied external load, the preload of the bolt and the way to subdivide the load between adhesive and bolt.

Stresses in x-direction (σ_x) showed maximum values at the overlap zone where the load transfer happened (Fig. 10a). Fig. 10b shows a side view of the stress field of the left side adherend due essentially to the joint rotation: compressive stresses occurred at the upper part and tensile stresses in the opposite part. Fig. 10c shows a compressive stress concentration due to the action exercised by the bolt during the contact.

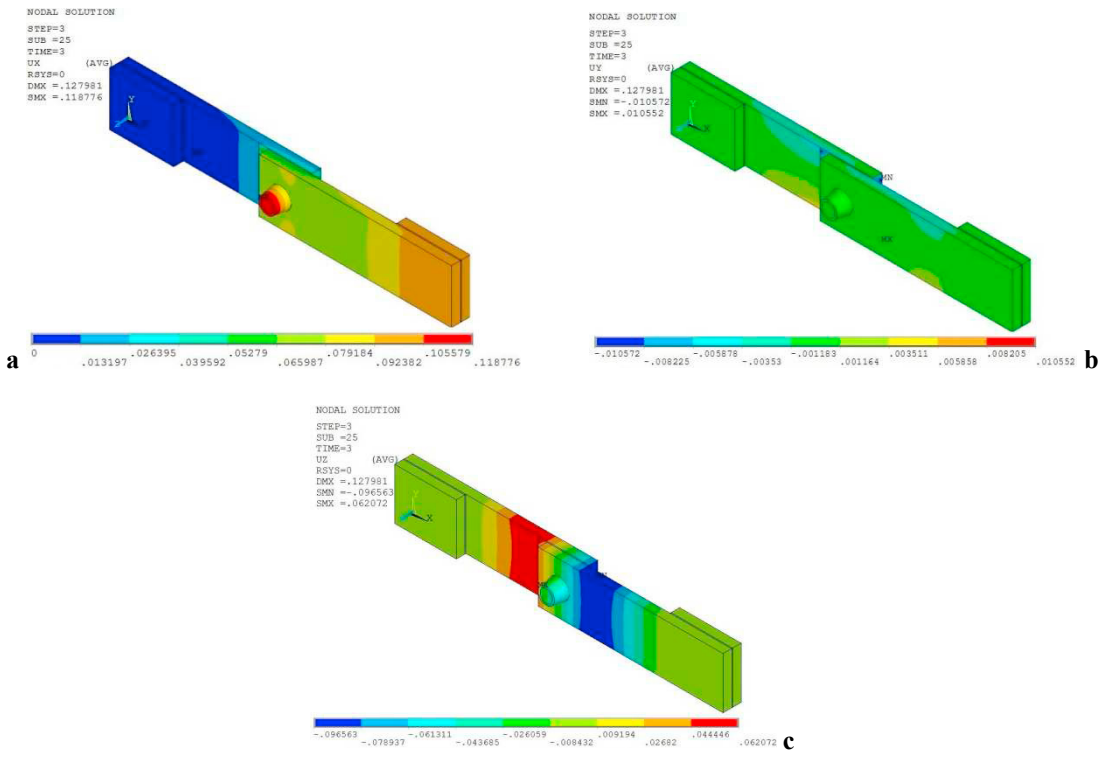

Fig. 9. (a) Displacement u_x [mm]; (b) displacement u_y [mm]; (c) displacement u_z [mm] (always for an applied external load of 3000 N).

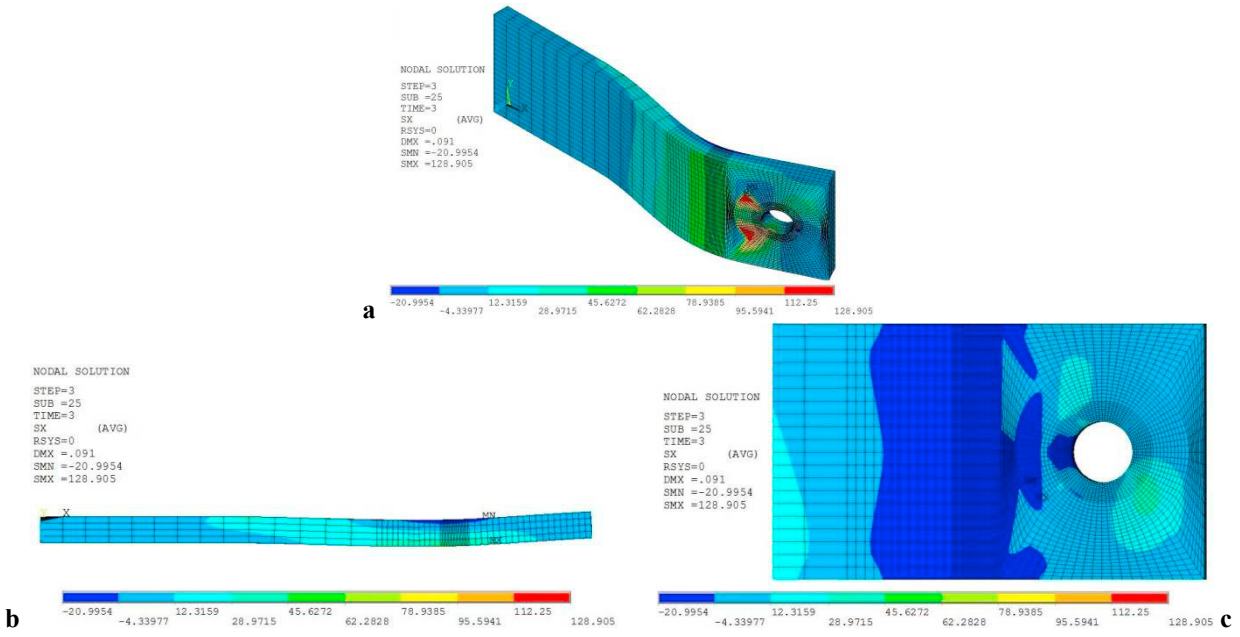

Fig. 10. (a) Stress field in x-direction (σ_x) [MPa] over the whole deformed shape of the left-side adherend; (b) side view of the stress σ_x [MPa] over the whole left-side adherend; (c) particular of the overlap zone (always for an applied external load of 3000 N).

Stresses in *y*-direction (σ_y) are symmetric as regards to the *xz* coordinate plane and are shown in Fig. 11.

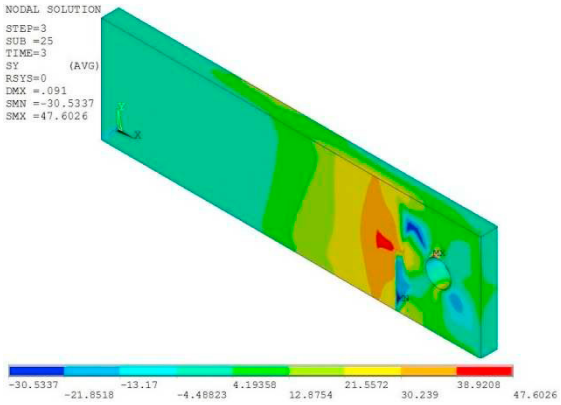

Fig. 11. Stress field in *y*-direction (σ_y) [MPa] (for an applied external load of 3000 N).

The stress in *z*-direction (σ_z) has remarkable values above all in the overlap zone (Fig. 12), particularly at the ends of this zone due to bending. The compression action of the preload is predominant in the zone under the bolt head where the compressive values are greater. Moreover the shear stresses in *xy* plane are shown in Fig. 13.

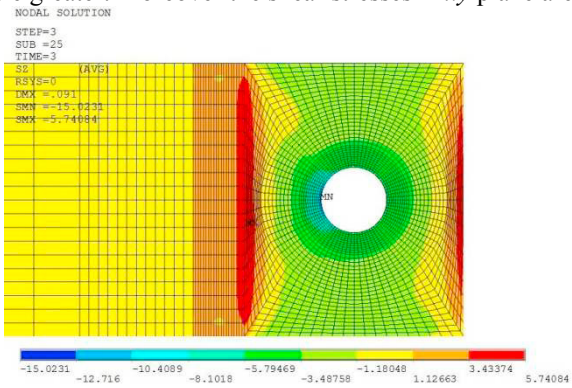

Fig. 12. Stress field in *z*-direction (σ_z) [MPa] (for an applied external load of 3000 N).

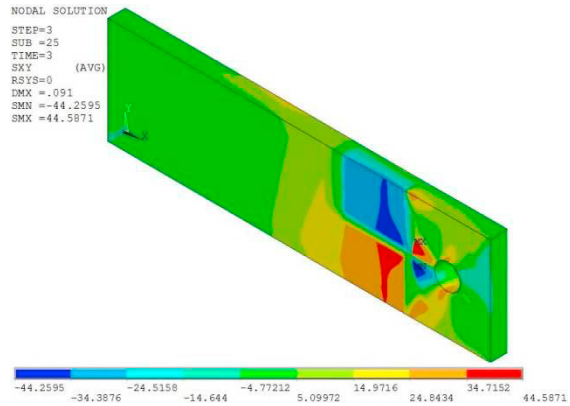

Fig. 13. Shear stress τ_{xy} [MPa] (always for an applied external load of 3000 N).

By evaluating the Von Mises equivalent stress, it was observed that the most stressed zone is the overlap one where the maximum value is 133.765 MPa (Fig. 14).

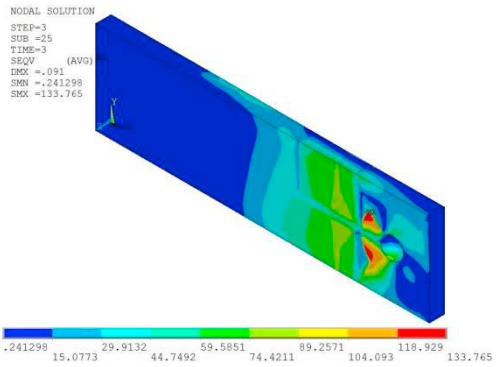

Fig. 14. Von Mises equivalent stress [MPa] (for an applied external load of 3000 N).

4.3. Adhesive

In a hybrid joint stresses acting on the adhesive layer are fundamentals because it is the lesser resistant component of the joint. Particular attention has to be paid to peel σ_z and shear τ_{xz} stresses; in fact the peel stress is the more detrimental stress for an adhesive due to its low normal stress resistance, whereas the shear stress influences the load transfer of the adhesive layer.

Fig. 15 shows the peel stress σ_z acting on the adhesive; it assumes maximum values near the edges of the overlap region, like a simply adhesive bonded joint, and then becoming negative (compression stress) near the hole due to preload.

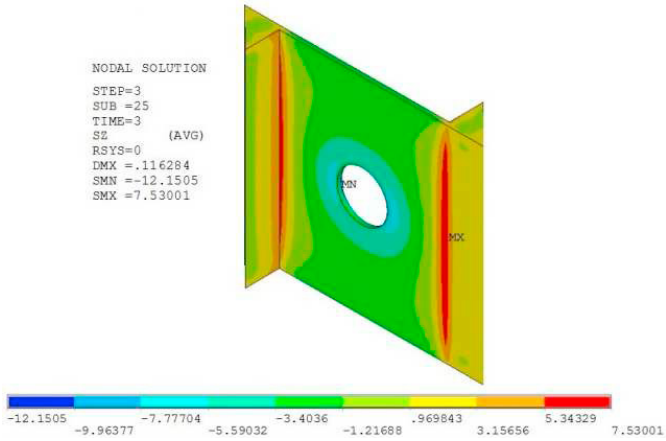

Fig. 15. Peel stress σ_z acting of the adhesive layer [MPa] (for an applied external load of 3000 N).

Fig. 16 shows the trend of the peel stresses σ_z evaluated in the middle plane (parallel to the *xz*-plane) of the adhesive layer along all the overlap length at the centre of the hole for both adhesive joint and hybrid joint for different applied external loads of 1000 N, 2000 N and 3000 N. The peaks of the peel stress are reached at the edges of the overlap zone and then reducing towards the overlap centre. However, in the case of hybrid joint the peel stress distribution decreases up to reach higher compressive values by approaching the hole due to preload. It was deduced that the presence of the preloaded bolt has an effect limited to the interaction surface at the bolt head and it reduces quickly departing from this zone.

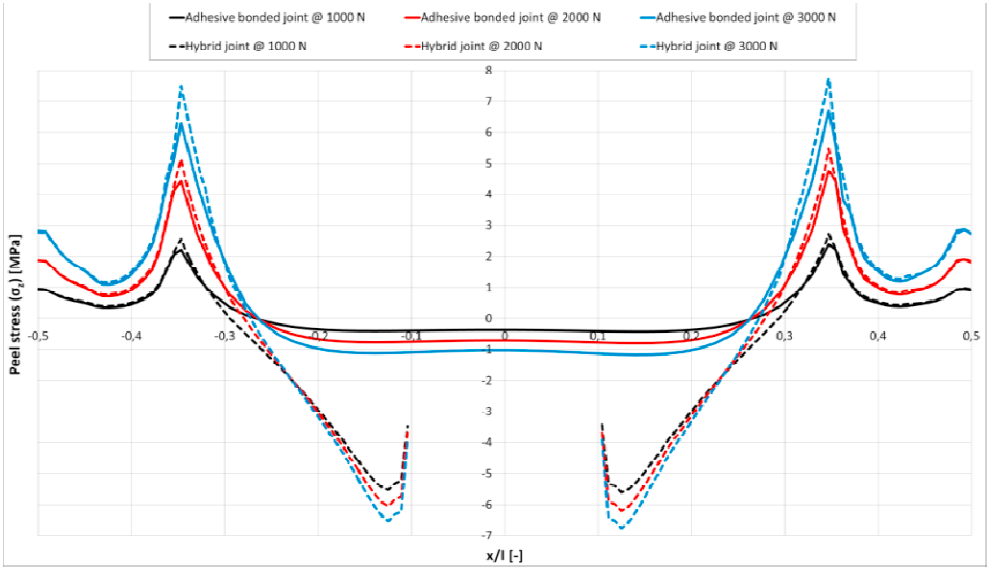

Fig. 16. Trend of the peel stress σ_z [MPa] in simply adhesive bonded joints and hybrid joints for the three applied external loads.

In Fig. 17 longitudinal (σ_x) and transverse (σ_y) stresses acting in the adhesive volume are shown.

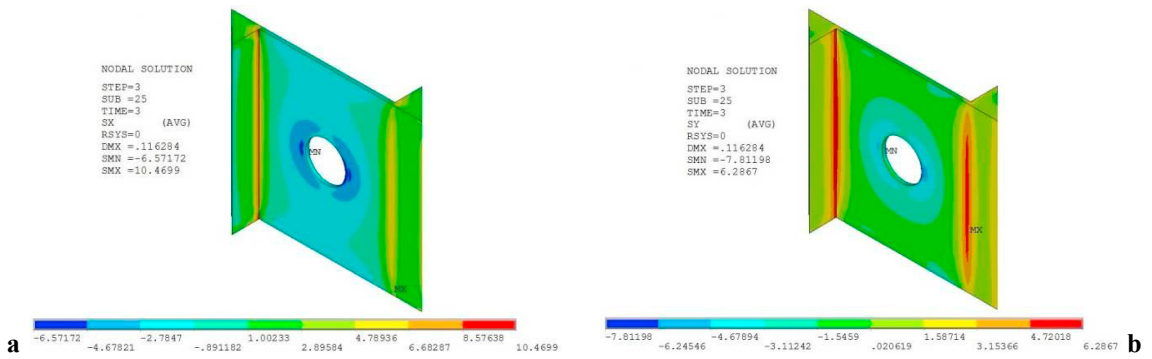

Fig. 17. (a) Longitudinal (σ_x) and (b) transverse (σ_y) stresses [MPa] acting on the adhesive volume (always for an applied external load of 3000 N).

Also the shear stress τ_{xz} showed peaks at the edges of the overlap zone and then reducing at the hole (Fig. 18).

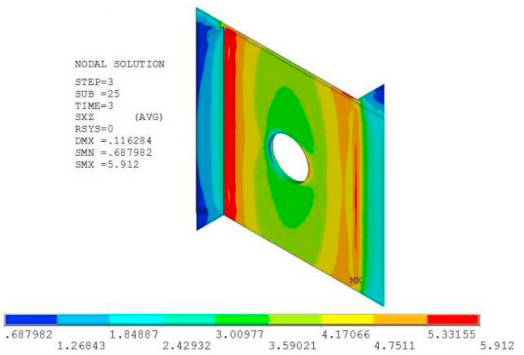

Fig. 18. Shear stress τ_{xz} [MPa] acting of the adhesive layer (for an applied external load of 3000 N).

Fig. 19 shows the trend of the shear stress τ_{xz} at the middle plane (parallel to the *xz*-plane) of the adhesive layer at the centre of the hole along the length of the overlap zone. Also in this case it is proposed a comparison between the stresses for simply adhesive bonded joints and hybrid joints at three different external load levels (1000 N, 2000 N and 3000 N). From the comparison of the two configurations, it can be noted a reduction of shear stresses τ_{xz} acting on hybrid joints due to the load transfer at the adhesive layer caused by the load transferred by the bolt. This reduction is less evident in cases of lower applied loads due to the lesser relative displacements obtained.

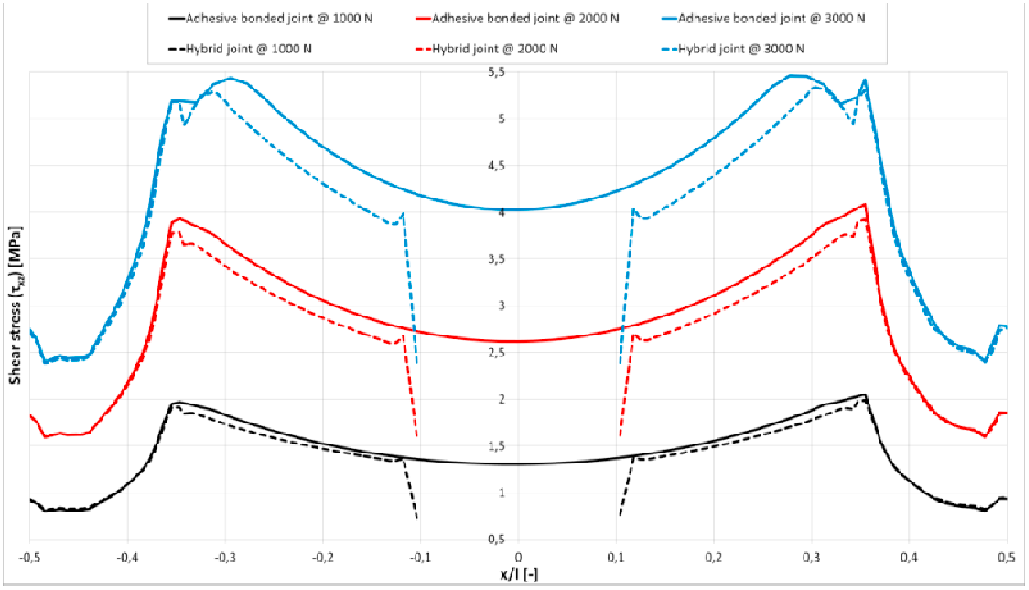

Fig. 19. Trend of the shear stress τ_{xz} [MPa] in adhesive bonded joints and hybrid joints for the three applied external loads.

Fig. 20 shows τ_{xy} and τ_{yz} shear stresses acting in the adhesive volume.

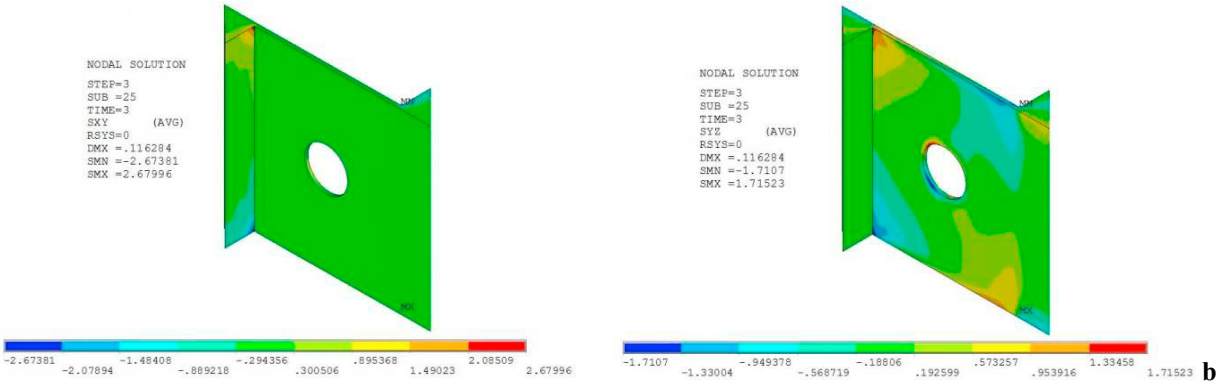

a **b**

Fig. 20. Shear stresses (a) τ_{xy} and (b) τ_{yz} [MPa] acting on the adhesive volume (always for an applied external load of 3000 N).

4.4. Bolt

The advantage due to the use of the bolt is based on its ability to transfer load. This ability depends on geometrical characteristics and material properties of the joint.

Basically the bolt is characterized by a tensile stress along its axis due to the preload (Fig. 21). From this figure it was observed that there were regions of stress concentration at the lateral surfaces of the shank because subjected to a greater elongation.

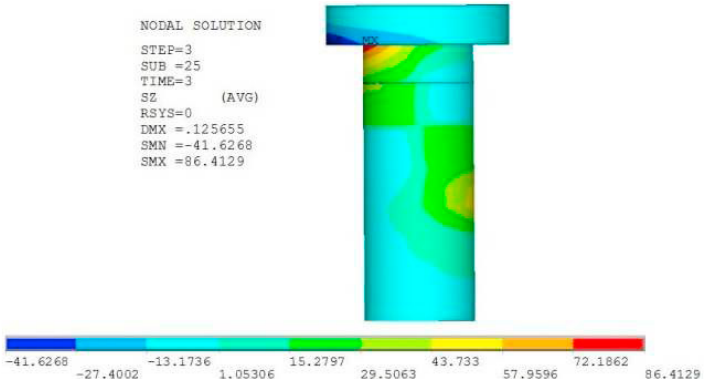

Fig. 21. Trend of the tensile stress in z-direction (σ_z) [MPa] acting on the bolt (for an applied external load of 3000 N).

The shear stress τ_{xz} acting on the bolt was due to the load transferred by it. Fig 22 shows the shear stress field obtained by sectioning the bolt at the position of the adhesive layer.

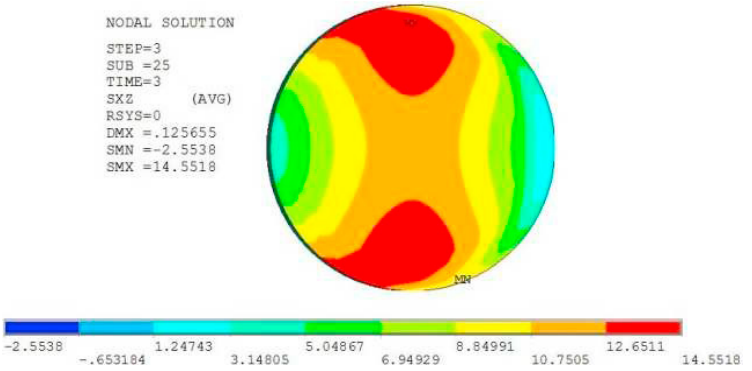

Fig. 22. Contour plot of the shear stress τ_{xz} [MPa] at the adhesive layer (for an applied external load of 3000 N).

The contact behaviour along the shank can be evaluated too (by selecting CONTA173 and TARGE170 elements). Fig. 23a shows the contact state. In correspondence of contact surfaces, the maximum contact pressure (Fig. 23b) and maximum friction stress (Fig. 23c) were obtained.

4.5. Load transferred by the bolt

The load transferred by the bolt can change considerably by varying the geometric characteristics and the mechanical properties of the joint components. In this work the variation of the load transferred by the bolt varying material yield stress, preload and applied external tensile load was evaluated.

Sensitivity analyses were made by using different values for tensile and shear yield stresses. Fig. 24 shows that the load transferred by the bolt in hybrid joints with different material properties of adhesive and different applied external load. The figure shows that the slope of curves are comparable until the external load is equal to 3000 N, after that the slope increases when the strength of adhesive decreases. This increase can be justified by the lower stiffness of the adhesive at big external loads which caused a quick rise of the load transferred by the bolt.

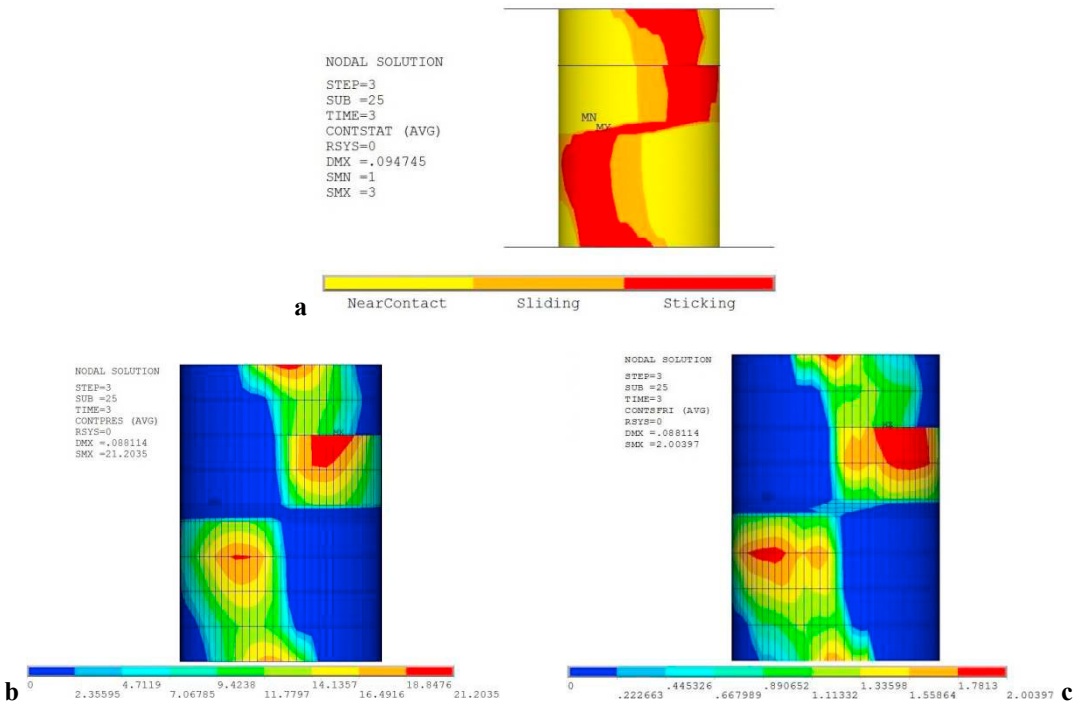

Fig. 23. (a) Contact status along the lateral surface of bolt's shank; (b) contact pressure and (c) friction stress acting on these surfaces (all for an applied external load of 3000 N).

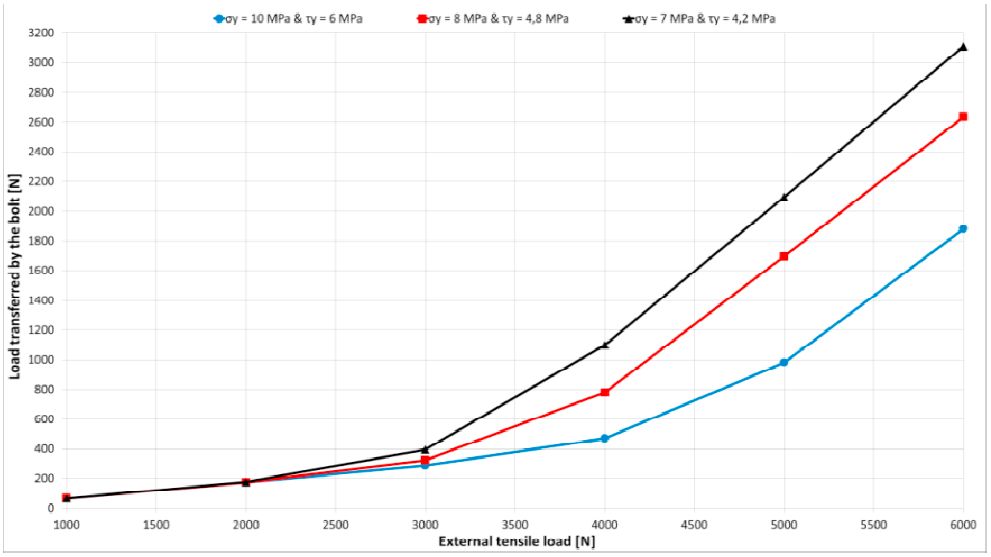

Fig. 24. Effect of the yield limits of the adhesive layer on the load transferred by the bolt vs. the external tensile load.

Also the value of the preload influences the transferred load: a greater value of the preload caused a reduction of the load transferred by the bolt. Sensitivity analysis was made with reference to preload values of 500 N and 5000 N (Fig. 25).

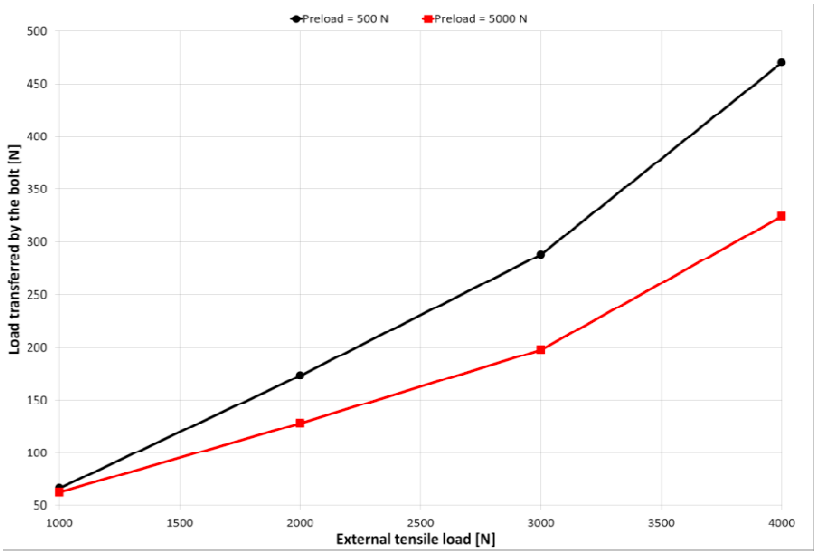

Fig. 25. Effect of the preload on the load transferred by the bolt vs. the external tensile load.

Finally, a two bolts configuration was analysed. Obviously the total load transferred by the two bolts was greater than that transferred in the one bolt case. This was due to the increase of the effective working section of the two bolts whereas that of the adhesive reduces. Fig. 26 compares the values obtained by the configurations with one and two bolts.

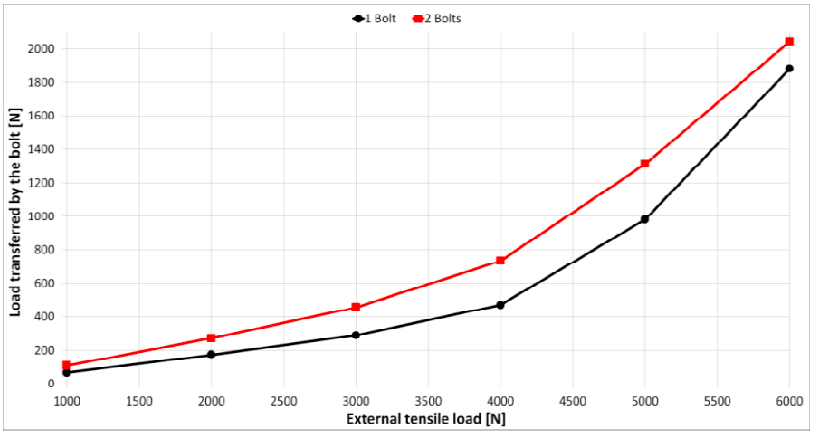

Fig. 26. Effect of number of bolts on the load transferred by the bolt vs. the external tensile load.

4.6. Experimental correlation

To validate the FEM simulation some experimental results found in Kelly (2005) were used. Values of the load transferred by the bolt were reported at 1000 N, 2000 N and 3000 N of external tensile load, by considering three different gaps between bolt's shank and hole (Fig. 27).

The numerical analysis points out a lesser load transfer when the gap increases; this is due to a greater relative displacement of the two laminates needed to close the gap and then to allow the bolt to work, though a lesser applied external tensile load was transferred.

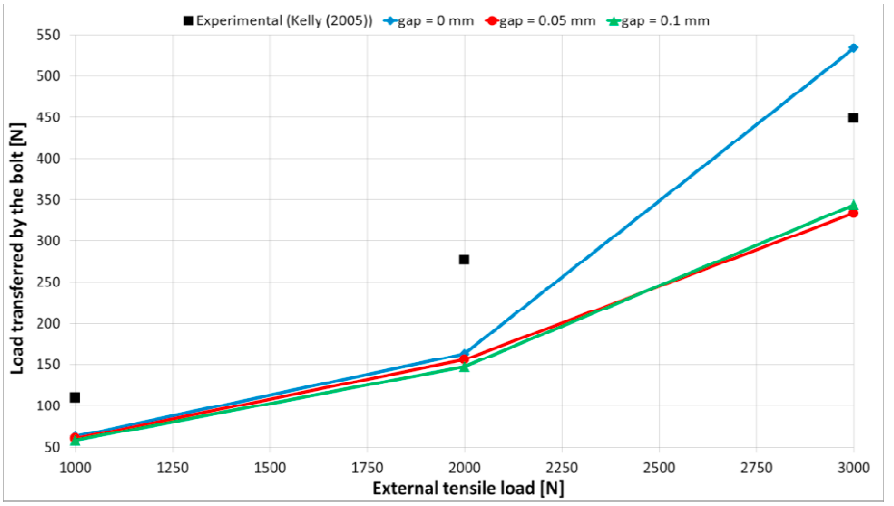

Fig. 27. Effect of the gap bolt-hole on the load transferred by the bolt vs. the external tensile load.

5. Conclusions

From numerical analyses it was observed that the use of the bolt allows to obtain a reduction of the shear stress acting on the adhesive layer in comparison of the simply adhesive bonded joint. However, as regards to the peel stress, there is not a reduction of the peak stress values because of the compression action induced by preload is limited in the range of the contact zone of the bolt head. Moreover, it was observed that the load transferred by the bolt increases when:

- the strength of the structural adhesive reduces;
- the preload acting on the bolt reduces;
- the gap between bolt's shank and hole reduces.

Finally, at the same load condition, the double bolt configuration allows to obtain a greater load transfer through the mechanical elements than the single bolt configuration.

References

ASTM D 638 - 02a, 2002. Standard test method for tensile properties of plastics. American Society for Testing and Materials.

Barroso, A., Vicentini, D., Mantič, V., París, F., 2010. Plasticity effects in CFRP-Al adhesive joints, 11th Pan-American Congress of Applied Mechanics, Foz do Iguaçu, Brazil.

Barut, A., Madenci, E., 2009. Analysis of bolted–bonded composite single-lap joints under combined in-plane and transverse loading, Composite structures 88, 579-594.

Crocombe, A.D., Ong, C.Y., Chan, C.M., Abdel Wahab, M.M., Ashcroft, I.A., 2002. Investigating fatigue damage evolution in adhesively bonded structures using backface strain measurement, The journal of adhesion 78, 745-776.

De Luca, A., Senatore, F., Greco, A., 2016. Numerical and experimental behaviour of adhesive joints subjected to peeling load, AIP Conference Proceedings 1736.

Hart-Smith, L.J., 1985. Bonded-bolted composite joints, Journal of aircraft 22, 993-1000.

Imanaka, M., Haraga, K., Nishikawa, T., 1995. Fatigue Strength of Adhesive/Rivet Combined Lap Joints, The journal of adhesion 49, 197-209.

Ireman, T., 1998. Three-dimensional stress analysis of bolted single-lap composite joints, Composite structures 43, 195-216.

Kelly, G., 2005. Load transfer in hybrid (bonded/bolted) composite single-lap joints, Composite structures 69, 35-43.

Kelly, G., 2006. Quasi-static strength and fatigue life of hybrid (bonded/bolted) composite single-lap joints, Composite structures 72, 119-129.

McCarthy, M.A., Lawlor, V.P., Stanley, W.F., McCarthy, C.T., 2002. Bolt-hole clearance effects and strength criteria in single-bolt single-lap, composite bolted joints, Composites science and technology 62, 1415–1431.

Paroissien, E., Sartor, M., Huet, J., 2007. Hybrid (Bolted/Bonded) joints applied to aeronautic parts: analytical one-dimensional models of a single-lap joint. In: Tichkiewitch S., Tollenaere M., Ray P. (Ed). Advances in Integrated Design and Manufacturing in Mechanical Engineering II. Springer, Dordrecht.